IEEE Access
Multidisciplinary | Rapid Review | Open Access Journal

Date of publication xxxx 00, 0000, date of current version xxxx 00, 0000.

Digital Object Identifier 10.1109/ACCESS.2017.Doi Number

Research on Inversion Model of Winding Hot Spot Temperature of 10kV Oil-immersed Three-dimensional Coiled Core Transformer

Qianyi Chen[1,2], Shaonan Chen[1], Weixiang Huang[1,2], Wei Zhang[1,2] and Kewen Li[1]

[1]Electric Power Research Institute of Guangxi Power Grid Company Limited, Nanning, 530023, China

[2]Guangxi Power Grid Equipment Monitoring and Diagnosis Engineering Technology Research Center, Nanning, 530023, China

Corresponding author: Weixiang Huang (huang_wx.sy@gx.csg.cn).

This work was supported the Science and Technology project of Guangxi Power Grid Company under Grant GXKJXM20220126.

ABSTRACT Realizing online monitoring of the hot spot temperature of grid mounted transformer windings is a challenge for the power industry. The heat exchange process between the internal heat source area and the external field area of the transformer is the direct cause of the temperature increase of the transformer shell. In this paper, based on the numerical coupling calculation of temperature - fluid field of 10kV oil immersed solid coiled iron core transformer, the typical heat flow streamline is extracted, and the measurable temperature characteristic points strongly correlated to the winding hot spot temperature are selected in the heat dissipation area of the shell, and the inversion model of the transformer winding hot spot temperature is established. This article verifies the effectiveness of the simulation results and the accuracy of the inversion model through the multi condition temperature rise test of transformer. The maximum error between the calculated steady-state temperature rise of each temperature measurement point in the simulation model and the test value is no more than 3°C, the simulation calculation results are in good agreement with the test results, and the average absolute error of the inversion model winding hot spot temperature inversion is 2.67 %, the maximum temperature difference is less than 3°C. This research provides an effective method for online monitoring of the hot spot temperature of the winding of a 10kV oil-immersed three-dimensional coil iron core transformer, and provides a reference for the state detection of grid mounted transformers.

INDEX TERMS oil-immersed transformer; temperature fluid field; streamline extraction; hot spot temperature inversion; power equipment status monitoring

I. INTRODUCTION

In transformer faults, the transformer damage rate caused by winding insulation failure is as high as 55.6% [1]. When the hot spot temperature of the transformer is less than 140℃, the insulation life is reduced to 1/2 of the original, and the insulation aging rate is doubled. Once the hot spot temperature of the transformer winding exceeds 140℃, the normal operation state of the transformer is broken, and the failure rate increases greatly [2], [3]. In order to ensure the safe and reliable operation of the transformer and reduce its insulation aging rate, it is necessary to pay attention to the hot spot temperature of the transformer. How to obtain the hot spot temperature of transformer windings has always been one of the difficulties that troubles the power industry. How to monitor the hot spot temperature of power transformers online and achieve status monitoring of power transformers is our goal.

Many researchers have carried out a lot of work on the calculation of transformer temperature distribution and hot spot temperature acquisition method. Transformer hot spot temperature acquisition methods mainly include direct measurement and indirect calculation methods. The direct measurement method is to install the optical fiber temperature sensor in the winding cake of the transformer or near the winding where overheating may occur for temperature acquisition [4], [5]. Indirect measurement methods mainly include empirical formula method, thermal path model method and numerical calculation method. The empirical formula method is to obtain the hot spot temperature of the winding from the temperature rise of the

measured top oil temperature relative to the top oil temperature. At present, the commonly used standards for calculating hot spot temperature of transformers are IEEE Standard C57.91-2001 [3]. The thermal circuit model method is to convert the thermal characteristic parameters to the electrical characteristic parameters, and realize the process of calculating hot spot temperature by using the equivalent model [6]. By establishing transformer model and using finite element integration method to solve boundary value problem, the numerical calculation method is simple and easy to operate. However, due to the complex structure of the transformer model and the existence of a large number of model grids in the dissection calculation, the calculation of the transformer temperature field is large and the calculation efficiency is low [7], [8].

Due to the complexity of the internal heat dissipation process during transformer operation, it is difficult to accurately describe the thermal characteristics of transformers using both direct measurement and indirect calculation methods. In addition, how to achieve online monitoring of the hot spot temperature of grid mounted transformers is a challenge that troubles the industry. In this context, the use of artificial intelligence algorithms to invert the temperature of hot spots based on transformer operation data has become a hot research topic today [9-11]. Artificial intelligence algorithms are mainly applied in two aspects, one of which is parameter optimization for empirical formulas or thermal path models. Due to the complex structure of transformers, although numerous key thermodynamic parameters are involved in existing empirical formulas and thermal calculation models, they are not sufficient to accurately describe the different heat dissipation characteristics of different transformers. Therefore, many scholars have introduced intelligent algorithms to optimize key thermodynamic parameters [12], [13]. The second is to directly construct the relationship between feature quantities and hot spot temperatures through artificial intelligence algorithms based on the collected transformer operation data. For example, some scholars have studied the application of neural network [14], support vector machine [15], fuzzy system [16] and Kalman filter algorithm [17] in transformer hot spot temperature prediction, and achieved good results.

However, in the current transformer hot spot temperature calculation model based on artificial intelligence algorithm, its input is based on the field operation data of transformer. During field operation, the hot spot temperature of the equipment will be affected by external factors. At the same time, due to the complexity of the transformer heat transfer process, the requirements for the establishment of training samples and input characteristic quantities of the prediction model are more stringent, and the input characteristic quantities selected according to production experience lack physical basis. The heat exchange process between the internal heat source area and the external field area of the transformer is the direct reason for the temperature rise of the transformer shell. For oil-immersed transformers, oil flow is the main medium for heat exchange. Based on the idea of heat flow coupling between the winding hot spot area and the shell heat dissipation area, the typical heat flow streamline can be extracted to obtain the shell temperature measurement points strongly related more effectively to the internal hot spot temperature [18], [19]. Therefore, the combination of streamline analysis method in temperature fluid field and artificial intelligence algorithm provides a new solution for transformer hot spot temperature inversion prediction.

In this paper, the 10kV oil-immersed three-dimensional coil core transformer is taken as the research object, and the law of heat exchange inside the transformer is analyzed by the numerical coupling calculation method of temperature-fluid field. Based on the idea of heat flow coupling between the winding hot spot area and the shell heat dissipation area, the typical heat flow streamline is extracted, and the measurable temperature characteristic points strongly related to the winding hot spot temperature are selected in the shell heat dissipation area. Considering the change of transformer load, a multi-feature training sample is constructed, and the nonlinear relationship between the multi-dimensional feature and the winding hot spot temperature is constructed based on the artificial intelligence algorithm, and the accuracy of the inversion prediction model is verified by the temperature rise test. The research provides an effective method for online monitoring of the hot spot temperature of the winding of 10kV oil-immersed three-dimensional coil iron core transformer, and provides a reference for the status detection of grid mounted transformers.

II. Temperature - fluid field calculation of transformer

A. Numerical coupling calculation method of transformer temperature and fluid field

1) TEMPERATURE - FLUID FIELD CONTROL EQUATION

The more mature method to solve fluid flow and heat transfer problems is CFD calculation method, which is based on three conservation laws: mass conservation law, momentum conservation law and energy conservation law, and is described by three conservation equations respectively [20].

Mass conservation equation:

$$\frac{\partial \rho}{\partial T} + div(\rho V) = 0 \tag{1}$$

Momentum conservation equation:

$$\begin{aligned}
&\frac{\partial(\rho u)}{\partial t} + div(\rho u V) = div(\mu \cdot gradu) - \frac{\partial p}{\partial x} + S_u \\
&\frac{\partial(\rho v)}{\partial t} + div(\rho v V) = div(\mu \cdot gradv) - \frac{\partial p}{\partial y} + S_v \\
&\frac{\partial(\rho w)}{\partial t} + div(\rho w V) = div(\mu \cdot gradw) - \frac{\partial p}{\partial z} + S_w
\end{aligned} \tag{2}$$

Energy conservation equation:

$$\frac{\partial(\rho T)}{\partial t} + div(pvT) = div\left(\frac{k}{C_P} div(T)\right) + \Phi + S_T \tag{3}$$

V is the fluid flow rate; u, v, w are the components of flow velocity in x, y and z directions; ρ Is the fluid density; μ Is the hydrodynamic viscosity; T is the fluid temperature; P is the fluid pressure; C_P is constant heat capacity; S_u, S_v, S_w are the generalized source terms of the momentum conservation equation; Φ is an internal heat source; S_T is viscous dissipation term.

2) BOUNDARY CONDITION CONTROL EQUATION

The external heat dissipation mainly depends on the heat convection along the surfaces of the transformer [21,22] . Heat flux q induced by external convection can be described by (4):

$$q = h_c S(T - T_f) \tag{4}$$

Where, T and T_f are the temperatures of the wall and the external fluid (air), S is the surface area of the wall, and h is the convective heat transfer coefficient, which are empirical parameters.

Heat convection coefficient h_c can be obtained from following equation:

$$h_c = a\mathrm{Ra}^b = \frac{\mathrm{Nu} \cdot k}{L} \tag{5}$$

where, Nu is the Nusselt number, Ra is Rayleigh number; a and b are constants determined by the system; L is the feature size; k is the thermal conductivity.

According to heat-transfer theory [21], the Nusselt number of vertical plane $\mathrm{Nu_v}$ and horizontal plane $\mathrm{Nu_h}$ can be analyzed by the following equations:

$$\begin{aligned} \mathrm{Nu_v} &= 0.59\mathrm{Ra}^{1/4} \\ \mathrm{Nu_h} &= 0.27\mathrm{Ra}^{1/4} \end{aligned} \tag{6}$$

The heat flux generated by the radiation heat transfer of the transformer shell can be represented by equation (7):

$$q = \sigma\varepsilon S F_{12}(T_1^4 - T_2^4) \tag{7}$$

ε is the emissivity, S is the surface area of the thermal radiation object, F_{12} is the shape coefficient from the radiation surface to the radiation surface, T_1 and T_2 are the temperatures of the thermal radiation object and the radiation object respectively.

By decomposing equation (7) according to equation (4), the unit area radiation heat transfer capacity of the transformer shell to the external environment can be equivalently expressed as the radiation heat transfer coefficient h_r, which is [21] :

$$\begin{aligned} h_r &= \frac{q}{(T_1 - T_2)} = \frac{\sigma\varepsilon S F_{12}(T_1^4 - T_2^4)}{(T_1 - T_2)} \\ &= \sigma\varepsilon S F_{12}(T_1^2 + T_2^2)(T_1 + T_2) \end{aligned} \tag{8}$$

Therefore, the heat dissipation intensity h of the oil immersed transformer shell can be expressed as the sum of the convection heat transfer coefficient h_c and the equivalent radiation heat transfer coefficient h_r under the conditions of Natural convection and forced commutation, which is:

$$h = h_c + h_r \tag{9}$$

B. Simulation model establishment and calculation parameter loading

1) SIMULATION MODEL ESTABLISHMENT

S13-M · RL-100 kVA/10 kV transformer is a three-phase three-column three-dimensional coil core transformer. Three-dimensional coil core transformer is an energy-saving power transformer, which changes the lamination magnetic circuit structure and winding layout of traditional power transformer. The product performance is more optimized, such as the three-phase magnetic circuit is completely symmetrical, the power saving effect is significant, the noise is greatly reduced, and the heat dissipation and overload capacity are stronger. The actual structure of S13-M · RL-100 kVA/10 kV transformer is shown in Fig 1, and the basic electrical parameters are shown in Table I.

TABLE I
S13-M · RL-100 KVA/10 KV BASIC PARAMETERS

Product model	S13-M·RL-100/10
Rated capacity	100 kVA
Voltage combination	10000±2×2.5%/400 V
Connection group	Dyn11
Cooling mode	ONAN
No-load loss	149.2 W
Load loss	1517.3 W(75℃)

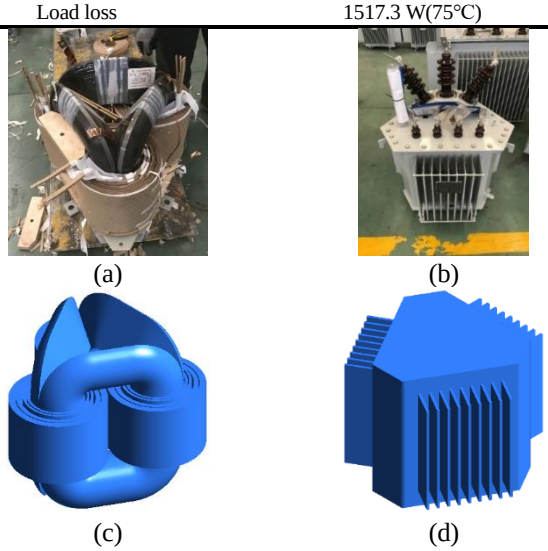

FIGURE 1. S13-M · RL-100 kVA/10 kV transformer. (a) Internal diagram of transformer (b) External drawing of transformer (c) Internal structure model (d) External structure model.

2) CALCULATION PARAMETER LOADING

The total loss of transformer includes core loss and load loss. The load loss consists of stray loss of structural parts and shell, resistance loss of high and low voltage windings, and eddy current loss of high and low voltage windings. The stray loss between the structure and the shell is obtained by calculating the transformer magnetic field. The resistance loss of high and low voltage windings is calculated based on the current of winding resistance. The eddy current loss of high and low voltage windings is distributed after the eddy current loss of high voltage and low voltage windings is determined based on the formula. The total loss P_n of transformer under other load rates is calculated as follows:

$$P_n = n^2 \times P_k + P_0 \quad (10)$$

Internal wall boundary conditions: Due to the existence of fluid viscosity, the relative velocity between the solid wall and the fluid near the wall is almost 0. Therefore, a non-slip boundary condition is set at the solid wall inside the transformer, and the wall temperature is consistent with the fluid temperature close to the wall.

Convective heat transfer coefficient of shell: In numerical simulation, the convective heat transfer coefficient is often used to equivalent the heat transfer process between the transformer and the external environment [23].

C. Temperature - fluid field calculation results

The finite volume method is used to calculate the temperature fluid field of the transformer, and the temperature distribution of S13-M • RL-100kVA/10kV transformer with 1.0 times the rated load under no wind condition is shown in Fig 2:

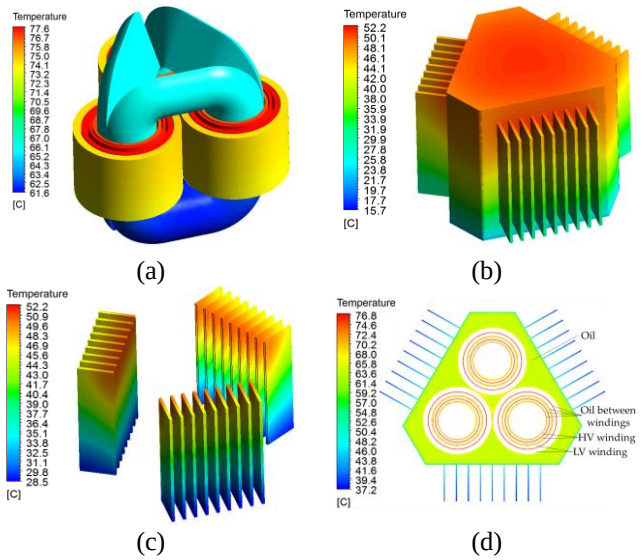

FIGURE 2. Temperature distribution inside transformer, shell and oil flow. (a) Transformer internal temperature distribution (b) Tank shell temperature distribution (c) Temperature distribution of heat sink (d) Section oil flow temperature distribution.

Because the transformer structure is symmetrical, and the heat dissipation conditions of the three-phase windings are the same, and the heat sources loaded by the three phases are the same, the temperature distribution of the transformer winding and iron core is basically symmetrical in three phases, and the temperature distribution of the three-phase windings is basically consistent with each other. The temperature of the transformer winding hot spot is 77.6°C, and the hot spot is located at the upper part of the high-voltage inner winding and the low-voltage outer winding, which is due to the narrow space of the distribution transformer, the internal oil channel of the transformer winding is narrow, and the heat dissipation condition is poor. The high voltage outer winding at the outer side has better heat dissipation conditions, and the temperature is significantly lower than the other three windings. The layer winding has no horizontal oil channel, and the winding can only dissipate heat through the adjacent vertical oil channel. The hot oil flows upward when heated, so the hot spot appears at the upper edge of the winding.

The overall oil flow of the transformer and the temperature distribution and oil flow of the winding oil passage are shown in Fig 3. The maximum oil flow velocity in the transformer occurs near the outlet of the longitudinal oil passage of the winding, and the flow velocity is about 0.024m/s. As the oil passage is narrow, the friction of solid wall affects the flow of oil flow, and the oil flow in the oil passage is slow, with the maximum flow rate of about 0.014m/s. The transformer oil flows through the winding oil duct and reaches the top layer after heating. The top layer hot oil flows into the radiator to form a regular laminar flow. After cooling by the radiator, it flows out of the radiator to enter the bottom layer of the transformer, and finally enters the winding oil duct to complete the oil flow cycle, which increases the heat dissipation efficiency. The oil flow at the corners of the transformer is very slow, forming a "quasi static oil zone", which basically does not participate in the whole oil flow circulation process. The winding hot spot appears at the upper end of the high voltage inner winding and the low voltage outer winding. The high voltage outer winding has the best heat dissipation conditions, the fastest external oil flow rate and the lowest corresponding temperature rise.

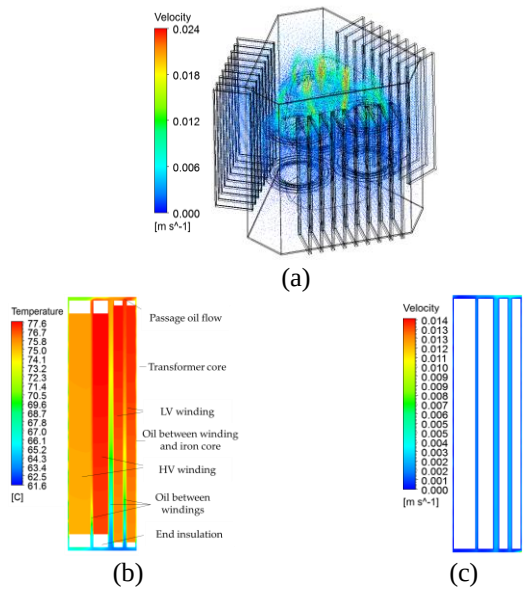

FIGURE 3. Oil flow velocity distribution under the condition of 1.0 times load and no wind. (a) Overall velocity distribution of transformer (b) Oil flow temperature distribution near winding (c) Distribution of oil flow velocity near winding.

In fluid motion, the trace refers to the trajectory of the fluid particle when it moves in space, and its tangent gives the velocity direction of the same fluid particle at different times. In the flow field, streamline refers to the curve that

each point is tangent to the fluid velocity vector, that is, streamline is a curve composed of different fluid particles at the same time, and the streamline gives the velocity direction of different fluid particles at that time. When the fluid motion reaches a steady state, the shape of the fluid streamline will no longer change with time, and the fluid streamline will coincide with the flow trace of the fluid moving particle [24]. Its particle trajectory equation is described as follows:

$$\frac{dX(t)}{dt} = \boldsymbol{v}(X(t)) = f(X(t), t) \tag{11}$$

The position of the next time step of the particle can be calculated by the above formula:

$$X_{k+1} = X_k + (t_{n+1} - t_n) \cdot \boldsymbol{v}(X_n) \tag{12}$$

Based on solving the particle trajectory equation, a main flow line in the transformer is calculated as shown in Fig 4.

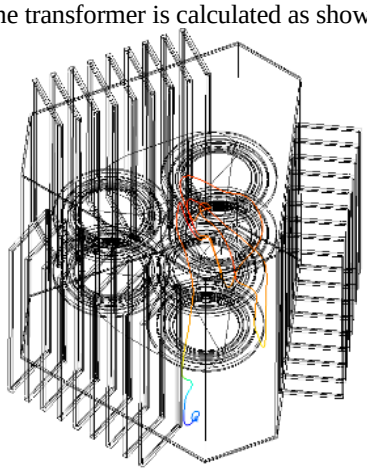

FIGURE 4. Main streamline inside transformer.

III. Inversion of transformer winding hot spot temperature

A. Extraction of characteristic temperature measurement points based on oil flow streamline

1) BASIC IDEA OF INVERSION

In the numerical coupling calculation of temperature-fluid field, the forward process is the process of calculating the overall temperature-fluid field distribution by loading the corresponding heat source excitation and boundary conditions on the simulation model. In this process, because the internal structure of the transformer is fixed and the material parameters are constant, the heat source excitation and boundary conditions applied jointly determine the temperature field distribution of the transformer shell. In addition, the heat exchange process calculated based on the same parameters also uniquely determines the temperature field distribution inside the transformer. The inverse calculation is based on the internal heat source and shell temperature to the transformer winding hot spot temperature [18], [19]. The overall idea is shown in Fig 5.

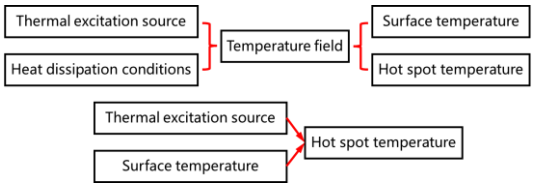

FIGURE 5. Hot spot temperature forward process and inversion.

For the transformer, the reason for its shell temperature rise is that the internal heat source of the transformer transfers heat to the external field through oil flow heat dissipation, and finally forms the overall temperature distribution of the transformer after stabilization. In the whole process, the heat exchange process based on oil flow directly leads to the overall temperature rise of the transformer. When there is no heat flow path between a hot spot of the transformer internal winding and a temperature measuring point of the shell, the temperature connection between the two points is weak, that is, when the temperature of the hot spot changes, the temperature of the temperature measuring point of the shell will not change. The objective of the inversion calculation in this paper is to build a multidimensional nonlinear mapping relationship between the characteristic quantity of the external field of the transformer and the temperature of the internal winding hot spot of the transformer. Therefore, selecting the external temperature measurement points that are strongly related to the temperature of the internal winding hot spot can ensure the mapping reliability and improve the inversion accuracy.

2) SELECTION OF SHELL FEATURE POINTS BASED ON OIL FLOW STREAMLINE

From the multi-physical field coupling analysis of S13-M • RL-100kVA/10kV transformer, the distribution of the main line inside the transformer can be obtained as shown in Fig 6. Three-phase winding of three-dimensional coil iron core, iron core structure and radiator position are completely symmetrical. The temperature of three-phase winding should be distributed symmetrically. The hot spot temperature can be obtained by analyzing the temperature of one phase winding. Since the location of the hot spot may appear in the low voltage winding or the high voltage winding, the observation of the streamline and the analysis of the main streamline passing through the hot spot and near the shell can be divided into two types: the cooling cycle through the heat sink and the cycle near the narrow corner.

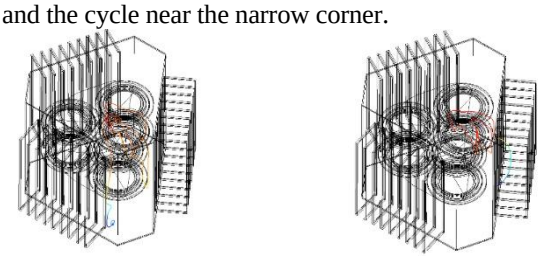

(a) (b)

FIGURE 6. S13-M · RL-100 kVA/10 main streamline inside transformer. (a) The first type of streamline (b) The second type of streamline.

Based on the analysis of the internal oil flow path of S13-M • RL-100kVA/10kV transformer, three characteristic temperature measuring points outside the transformer are selected, and the specific location distribution is shown in Table II.

TABLE II
ARRANGEMENT OF TEMPERATURE MEASURING POINTS OF TRANSFORMER SHELL

Temperature measuring point number	Temperature measuring point position
1#	Transformer top oil temperature measurement position
2#	Oil flow inlet of transformer phase A radiator
3#	Oil flow inlet of transformer phase B radiator

B. Support Vector Regression (SVR)

1) BASIC PRINCIPLES OF SUPPORT VECTOR REGRESSION (SVR)

The basic principle of support vector regression (SVR) is as follows [25], [26]:

For a set of training data, (X_j,Y_j), j=1,2,…,M, $X_j \in R_N$, $Y_j \in R$. To describe the nonlinear relationship between input X and output Y, it is assumed that there is a hyperplane:

$$G(X)=\Omega \cdot X+B \tag{13}$$

The hyperplane satisfies the following formula:

$$|Y_j-G(X_j)|\leqslant \epsilon\ ,\ j=1,2,...,M \tag{14}$$

In the above formula, ε is the insensitive loss coefficient.

In the training data, the distance from any point to the hyperplane is calculated by the following formula:

$$D_j=\frac{|\Omega \cdot X_j+B-Y_j|}{\sqrt{1+\|\Omega\|^2}}\leqslant\frac{\epsilon}{\sqrt{1+\|\Omega\|^2}} \tag{15}$$

When the distance between the training data and the hyperplane is the smallest, the hyperplane is the optimal hyperplane. The solution of the optimal hyperplane can be expressed by the following formula:

$$\begin{cases}\min\ \Phi(\Omega)=\dfrac{1}{2}\|\Omega\|^2\\ s.t.\ \ |\Omega \cdot X_j+B-Y_j|\leqslant\epsilon\end{cases} \tag{16}$$

The relaxation variables ζ and Lagrange multipliers v_i and v_i^* are introduced to solve the above equations, and the expression of the optimal hyperplane is obtained as follows:

$$G(X)=\sum_{j=1}^{M}(v_i-v_i^*)K(X_j,X)+B \tag{17}$$

In the above formula, $K(X_j,X)$is the kernel function. Based on the advantages of RBF kernel function in nonlinear mapping, the expression of RBF kernel function is selected as follows:

$$K(X_j,X_i)=EXP\left(-\gamma\|X_j-X_i\|^2\right) \tag{18}$$

In the above formula, γ is the kernel function parameter, γ>0.

2) PARAMETER OPTIMIZATION AND EVALUATION INDEX

In this paper, the K-fold cross-validation algorithm is used to optimize the penalty coefficient C and kernel function parameter γ of the support vector regression machine. The K-fold cross-validation algorithm divides the training sample data set into K parts, and uses the K-1 group of data in each test, and uses the remaining group of data as the test sample to conduct K tests.

In the algorithm training, the grid search (GS) parameter optimization method is used to find the optimal parameters of SVR model. The grid search method is to map the penalty coefficient and kernel function parameters that need to be optimized to the XOY two-dimensional plane, and at the same time specify the search range and step size of the penalty coefficient and kernel function parameters to divide the plane into two-dimensional grids. During the training process, a set of penalty coefficients and kernel function parameters mapped by each grid node are substituted into the SVR model, and the combination with the highest accuracy will become the best parameters of the inversion model [27], [28].

In order to verify the effect of the model, SSE, MAPE and MSPE are used to evaluate the effect of the model. The formula is as follows:

$$\begin{cases}SSE=\sum_{i=1}^{N}(S_i-O_i)^2\\ MAPE=\dfrac{1}{N}\sum_{i=1}^{N}\left|\dfrac{S_i-O_i}{S_i}\right|\\ MSPE=\dfrac{1}{N}\sqrt{\dfrac{1}{N}\sum_{i=1}^{N}\left(\dfrac{S_i-O_i}{S_i}\right)^2}\end{cases} \tag{19}$$

In the above formula, S is the simulation value, O is the inversion value, i is the sample number, and N is the total number of samples.

C. Establishment of inverse model of transformer winding hot spot temperature

1) TRAINING SAMPLE ESTABLISHMENT

In this paper, the common orthogonal test method is used to design the training samples of the inversion model, and the load rate and environmental conditions are comprehensively considered [29]. After screening various environmental factors, wind speed, temperature, and humidity, which have a significant impact on the environment, were ultimately selected as the environmental factors required for constructing the sample. The parameters of the four-factor three-level orthogonal table required for the design are shown in Table III:

TABLE III
4 FACTORS 3 HORIZONTAL ORTHOGONAL TABLE PARAMETERS.

level	Load rate	Wind speed(m/s)	Temperature(˚C)	Humidity(%)
1	0.6	0	0	20
2	1.0	2	15	40
3	1.3	4	30	60

According to the above parameters, corresponding to the 4-factor 3-level orthogonal test table, the orthogonal training samples are designed as shown in Table IV:

TABLE IV
4-FACTOR 3-LEVEL ORTHOGONAL TEST TABLE (TRAINING SAMPLE)

No.	Load rate	Wind speed(m/s)	Temperature(˚C)	Humidity(%)
1	0.6	0	30	20
2	0.6	2	15	40
3	0.6	4	0	60
4	1.0	0	50	60
5	1.0	2	0	20
6	1.0	4	30	40
7	1.3	0	0	40
8	1.3	2	30	60
9	1.3	4	15	20

The designed orthogonal test samples of 4 factors and 3 levels are shown in Table V:

TABLE V
4-FACTOR 3-LEVEL ORTHOGONAL TEST TABLE (TEST SAMPLE)

No.	Load rate	Wind speed(m/s)	Temperature(˚C)	Humidity(%)
1	0.52	0.5	6	18
2	0.63	1.2	2	36
3	0.76	0.7	11	44
4	0.81	1.1	7.5	18
5	0.95	1.8	5	28
6	1.02	2.4	16	38
7	1.13	1.5	9	40
8	1.26	2.8	10	16

2) INVERSION RESULTS OF WINDING HOT SPOT STEADY-STATE TEMPERATURE

Take the sum of three-phase maximum load rate, three-phase minimum load rate and three-phase load rate as the load characteristic quantity, take the temperature of the characteristic temperature measuring point of the shell as the temperature characteristic quantity, take the winding hot spot temperature as the output, and construct the transformer winding hot spot temperature inversion model through support vector regression (SVR).

The grid search method is used for parameter optimization, in which penalty coefficient C and kernel function are set γ. The search range of is $[2^3,2^{17}]$ and $[2^{-15},2^{-8}]$, the discount *v* of cross validation is 9, and the non-sensitive loss coefficient ε is 10^{-2}. The fitness curve of the training sample is shown in Fig 7.

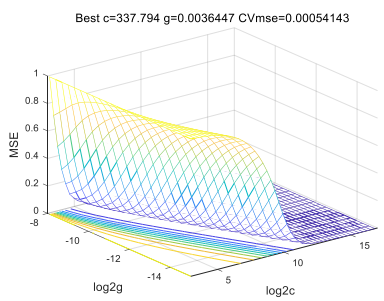

FIGURE 7. SVR model parameters optimized by GS.

The optimization results of the kernel function parameters under GS algorithm and the three error indicators of the corresponding test sample winding hot spot inversion are shown in Table VI.

TABLE VI
PARAMETER OPTIMIZATION RESULT OF GS ALGORITHM AND ERROR INDEX OF TEST SAMPLE

Parameter	Value	Parameter	Value
C	337.79	e_{SSE}	69.28
γ	3.64×10^{-3}	e_{MAPE}	2.67×10^{-2}
t/s	2.79	e_{MSPE}	6.91×10^{-3}
Fitness	5.41×10^{-4}		

Substitute the optimal parameters into the SVR model to invert the winding hot spot temperature of the test sample in Table 4. Compare the inversion results with the measured and calculated values respectively. See Table VII for the inversion results. In order to verify the effectiveness of the proposed inversion method of hot-spot temperature of oil-immersed transformer winding based on streamline morphology analysis and support vector regression machine in S13-M • RL-100kVA/10kV transformer hot-spot steady-state temperature inversion, this section uses the empirical formula recommended by the standard to calculate the hot-spot temperature of 8 groups of test samples. The inversion results of GS-SVR proposed in this paper and the calculation results of empirical formula are compared with the experimental values or the calculation values of multi-physical field coupling model.

TABLE VII
INVERSION OF CALCULATION RESULTS USING GS-SVR

No.	CV(˚C)	GS-SVR		Empirical formula	
		IV(˚C)	TD(˚C)	IV(˚C)	TD(˚C)
1	34.1	36.25	-2.15	34.51	-0.41
2	37.8	38.91	-1.11	38.12	-0.32
3	55.1	55.27	-0.17	57.32	-2.22
4	55.6	54.91	0.69	58.07	-2.47
5	63.4	61	2.4	68.38	-4.98
6	75	72.95	2.05	86.27	-11.27
7	79.4	76.62	2.78	90.71	-11.31
8	85.8	83.25	2.55	105.15	-19.35

CV is calculated value of hot spot temperature, IV is inversion value, TD is temperature difference.

It can be seen from the above inversion results that GS-SVR has achieved good results in the inversion of test samples, with the maximum temperature difference less than 3℃ and the maximum absolute percentage error of 6.0%. The temperature difference calculated by empirical formula method is large, and the temperature difference exceeds 15℃ in some cases.

IV. Inversion model test verification

A. Transformer temperature rise test

In this test, FTM-6CH-H200 optical fiber thermometer is used to measure the hot spot temperature of the transformer winding, which is respectively arranged in the oil channel between the phase A, phase B and phase C high voltage winding and low voltage winding of the transformer. The

actual layout of optical fiber temperature measuring points is shown in Fig 8.

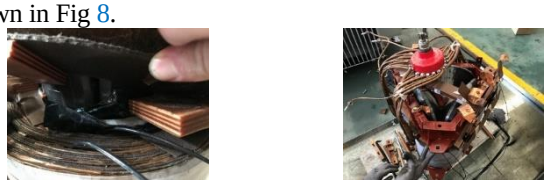

(a) (b)

FIGURE 8. Layout of optical fiber thermometer. (a) Optical fiber embedded winding (b) Overall arrangement.

The shell temperature measurement point is very important for the inversion of the hot spot temperature of the transformer. This test uses PT1000 thermal resistance to monitor the shell temperature. The temperature measuring points are arranged at the typical points in the transformer temperature rise distribution to ensure the validity of the data measured at the temperature measuring points. Three temperature measuring points are arranged on the oil tank shell. Table VIII shows the arrangement of three thermal resistance temperature measuring points.

TABLE VIII
LAYOUT OF THERMAL RESISTANCE TEMPERATURE MEASURING POINTS

Temperature measuring point	Layout location
L1	Outer wall top shell center
L2	1/3 height of narrow side of outer wall
L3	Bottom of narrow edge of outer wall

The actual arrangement of thermal resistance is shown in Fig 9.

FIGURE 9. Arrangement of thermal resistance temperature measurement system.

B. Analysis of temperature rise test results

1) COMPARISON AND ANALYSIS OF TEMPERATURE FIELD CALCULATION RESULTS AND TEST RESULTS UNDER MULTIPLE WORKING CONDITIONS

The loading conditions for the temperature rise test of S13-M • RL-100kVA/10kV three-phase three-column stereoscopic coil core transformer are shown in Table IX.

TABLE IX
TEMPERATURE RISE TEST LOADING CONDITIONS

No.	LM	WS	No.	LM	WS
1	1.0	0m/s	7	0.9	3m/s
2	0.7	0m/s	8	1.2	3m/s
3	0.9	0m/s	9	0.8	2m/s
4	1.2	0m/s	10	1.1	2m/s
5	0.8	0m/s	11	0.7	1m/s
6	1.1	0m/s	12	1.0	1m/s

LM is Load loss multiple, WS is Wind speed.

The above model is used to calculate the steady-state test conditions in this test. The comparison between the calculated results of steady-state temperature rise and the test results is shown in Table X.

TABLE X
COMPARISON OF TEMPERATURE RISE CALCULATION AND TEST RESULTS

No.	TV/CV	MT (℃)				AT
		HST	L1	L2	L3	
1	TV	56.8	35.0	32.4	17.0	10.0
	CV	56.4	35.9	32.0	17.6	
2	TV	66.1	42.2	40.3	21.9	15.0
	CV	66.5	45.8	42.0	23.8	
3	TV	75.7	50.3	48.2	25.1	14.8
	CV	74.7	52.6	48.8	23.2	
4	TV	78.9	50.7	47.7	21.4	10.7
	CV	77.6	52.4	48.3	23.5	
5	TV	91.8	65.0	60.7	31.0	16.0
	CV	90.0	64.4	60.7	28.7	
6	TV	94.6	62.8	60.7	27.5	12.2
	CV	93.0	64.2	60.4	29.1	
7	TV	52.9	28.3	26.4	13.6	12.0
	CV	53.5	30.8	27.1	15.2	
8	TV	58.4	32.9	29.6	14.9	10.0
	CV	57.8	34.0	29.4	14.1	
9	TV	64.5	36.7	33.1	18.1	16.3
	CV	66.0	38.5	34.1	19.8	
10	TV	69.5	39.6	34.1	11.9	9.0
	CV	70.5	39.1	34.2	14.6	
11	TV	76.8	44.7	39.8	15.7	10.0
	CV	77.4	46.5	40.9	16.8	
12	TV	83.8	50.4	45.6	19.8	13.5
	CV	82.2	47.9	42.7	19.1	

TV is test value, CV is calculated value, MT is monitoring point temperature, HST is measured value of hot spot temperature, AT is ambient temperature. L1, L2, L3 is the arrangement of three thermal resistance temperature measuring points in Table VIII.

It can be seen from Table X that the maximum error between the calculated value and the test value of each temperature measurement point in the calculation of steady-state temperature rise is not more than 3℃. The simulation results are in good agreement with the test results, indicating that the calculation model can accurately obtain the temperature distribution of S13-M • RL-100kVA/10kV transformer winding and shell under different load current, wind speed and ambient temperature conditions through multi-physical field coupling calculation.

2) VERIFICATION OF STEADY-STATE HOT SPOT TEMPERATURE INVERSION MODEL

Based on the inversion model of winding hot spot temperature obtained from the above training, 12 groups of steady-state temperature rise test conditions in the transformer temperature rise test are taken as test samples to

invert the winding steady-state hot spot temperature under the actual test conditions. In order to compare with this paper, the empirical formula recommended in IEEE Standard C57.91-2001 [3] is used to calculate the steady-state hot spot temperature of windings under 12 inter-group test conditions. In addition, the calculation results, inversion values and test values are compared, and the comparison results are shown in Table XI.

TABLE XI
INVERSION OF TEST RESULTS USING GS-SVR

No.	HST(˚C)	GS-SVR		Empirical formula	
		IV(˚C)	TD(˚C)	IV(˚C)	TD(˚C)
1	78.9	77.04	1.86	78.97	-0.07
2	56.8	54.72	2.08	51.45	5.35
3	75.7	73.88	1.82	73.46	2.24
4	94.6	93.39	1.21	101.56	-6.96
5	66.1	64.24	1.86	64.70	1.40
6	91.8	90.7	1.1	94.51	-2.71
7	64.5	63.63	0.87	74.96	-10.46
8	83.8	83.58	0.22	102.86	-19.06
9	58.4	56.54	1.86	59.70	-1.30
10	76.8	75.24	1.56	89.01	-12.21
11	52.9	49.7	3.2	53.45	-0.55
12	69.5	67.36	2.14	78.27	-8.77

HST is measured value of hot spot temperature, IV is inversion value, TD is temperature difference.

The calculation error is shown in Fig 10, and the calculation results of various error indicators are shown in Table XII.

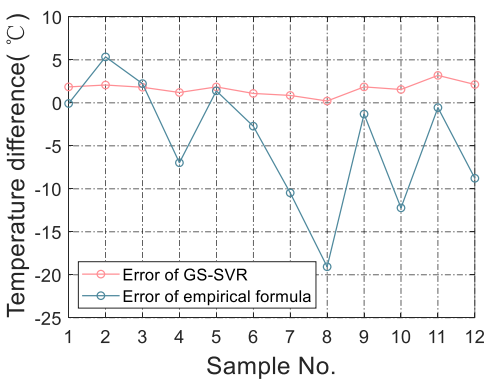

FIGURE 10. Comparison of inversion error and empirical formula calculation error.

TABLE XII
ERROR INDEX OF GS-SVR AND EMPIRICAL FORMULA CALCULATION RESULTS

Result	GS-SVR	Empirical formula
e_{SSE}	69.28	1496.99
e_{MAPE}	2.67×10-2	8.35×10-2
e_{MSPE}	6.91×10-3	2.58×10-2

GS-SVR has achieved good results in the inversion of test samples, with the maximum temperature difference less than 3.2℃ and the maximum absolute percentage error of 6.0%. The temperature difference calculated by empirical formula method is large, and the temperature difference exceeds 15℃ in some cases.

V. Conclusion

In this paper, S13-M • RL-100kVA/10kV oil-immersed stereoscopic coil core transformer is taken as the research object, and the temperature-fluid field distribution of 10kV oil-immersed stereoscopic coil core transformer under different working conditions is studied using the numerical coupling calculation method of temperature-fluid field. The heat exchange process based on oil flow inside the transformer is analyzed, and the characteristic temperature extraction points on the transformer shell with strong correlation with the winding hot spot temperature are selected by extracting the heat flow path. Considering the load rate and environmental factors of the transformer during operation, the multidimensional nonlinear relationship between the characteristic quantity and the winding hot spot temperature is constructed by using the support vector regression (SVR) model, and the winding hot spot temperature inversion model of 10kV oil-immersed three-dimensional coil core transformer is developed. The maximum error between the calculated value of each temperature measuring point and the test value is not more than 3 ℃, and the simulation calculation results are in good agreement with the test results, indicating that the calculation model can accurately obtain the temperature distribution of S13-M · RL-100kVA/10kV transformer winding and housing under different load current, wind speed and ambient temperature conditions through Multiphysics simulation coupling calculation.

Combined with the steady state temperature rise test of 10kV oil-immersed stereoscopic coil core transformer, the test sample of inversion model is constructed. By comparing with the winding hot spot temperature calculated by empirical formula, the accuracy of inversion model is verified. The maximum error of inversion is 3.2℃, and the maximum absolute error percentage is 6.05%. Good inversion effect is achieved. The inversion accuracy is better than that calculated by empirical formula. At the same time, the research content of this paper has good universality for oil-immersed three-dimensional coil core transformer. The research content of this article provides an effective method for online monitoring of the hot spot temperature of the winding of 10kV oil-immersed three-dimensional coil iron core transformer, and provides a reference for the status detection of grid mounted transformers.

REFERENCES

[1] Y. S. Quan, Z. S. Ning, S. Y. Chen, W. Li and T. Y. Xu, "Study on the methodology of detection for transformer winding insulation defects based on applied voltage test," *2012 IEEE International Symposium on Electrical Insulation*, San Juan, PR, USA, 2012, pp. 153-155.

[2] B. Garcia, J. C. Burgos and A. M. Alonso, "Transformer tank vibration modeling as a method of detecting winding deformations-

part I: theoretical foundation," in *IEEE Transactions on Power Delivery*, vol. 21, no. 1, pp. 157-163, Jan. 2006.

[3] Power Transformers —Part 7: Loading guide for oil-immersed power transformers. IEC Standard 60076-7, 2005.

[4] M. P. Saravolac, "The use of optic fibres for temperature monitoring in power transformers," *IEE Colloquium on Condition Monitoring and Remanent Life Assessment in Power Transformers*, London, UK, 1994, pp. 7/1-7/3.

[5] W. J. McNutt, J. C. McIver, G. E. Leibinger, D. J. Fallon and K. A. Wickersheim, "Direct Measurement of Transformer Winding Hot Spot Temperature," in *IEEE Transactions on Power Apparatus and Systems*, vol. PAS-103, no. 6, pp. 1155-1162, June 1984.

[6] Montsinger, Cooney, Doherty and Carter, "Temperature rise of stationary electrical apparatus as influenced by radiation, convection and altitude: Effect of altitude on temperature rise," *J. Am. Inst. Electr. Eng.*, vol. 44, no. 3, pp. 283–288, Mar. 1925.

[7] R. Gong, J. Ruan, J. Chen, Y. Quan, J. Wang, and S. Jin, "A 3-D Coupled Magneto-Fluid-Thermal Analysis of a 220 kV Three-Phase Three-Limb Transformer under DC Bias," in *Energies*, vol. 10, no. 4, p. 422, Mar. 2017.

[8] R. Gong, J. Ruan, J. Chen, Y. Quan, J. Wang, and C. Duan, "Analysis and Experiment of Hot-Spot Temperature Rise of 110 kV Three-Phase Three-Limb Transformer," in *Energies*, vol. 10, no. 8, p. 1079, Jul. 2017.

[9] G. B. Wolff, H. . -J. Haubrich and T. Seitz, "Evaluation of nonsteady loading limits for network components using artificial neural networks," *1993 2nd International Conference on Advances in Power System Control, Operation and Management, APSCOM-93.*, Hong Kong, 1993, pp. 355-360 vol.1.

[10] T. J. Hammons, "Artificial intelligence in power system engineering: Actual and potential applications of expert systems, knowledge-based systems, and artifical neural networks," in *IEEE Power Engineering Review*, vol. 14, no. 2, pp. 11-, February 1994.

[11] T. Nogami, Y. Yokoi, H. Ichiba and Y. Atsumi, "Gas discrimination method for detecting transformer faults by neural network," *Proceedings of 1994 IEEE International Conference on Neural Networks (ICNN'94)*, Orlando, FL, USA, 1994, pp. 3800-3805 vol.6.

[12] D. Villacci, G. Bontempi, A. Vaccaro and M. Birattari, "The role of learning methods in the dynamic assessment of power components loading capability," in *IEEE Transactions on Industrial Electronics*, vol. 52, no. 1, pp. 280-290, Feb. 2005.

[13] GALDI V, IPPOLITO L, PICCOLO A. Parameteridentification of power transformers thermal model viagenetic algorithms[J]. Electric Power Systems Research,2001, 60(2): 107-113.

[14] E. A. Juarez-Balderas, J. Medina-Marin, J. C. Olivares-Galvan, N. Hernandez-Romero, J. C. Seck-Tuoh-Mora and A. Rodriguez-Aguilar, "Hot-Spot Temperature Forecasting of the Instrument Transformer Using an Artificial Neural Network," in *IEEE Access*, vol. 8, pp. 164392-164406, 2020.

[15] Y. Cui, H. Ma and T. Saha, "Transformer hot spot temperature prediction using a hybrid algorithm of support vector regression and information granulation," *2015 IEEE PES Asia-Pacific Power and Energy Engineering Conference (APPEEC)*, Brisbane, QLD, Australia, 2015, pp. 1-5.

[16] H. Matsila and P. N. Bokoro, "Insulation Life Loss Prediction of an Oil-Filled Power Transformer Using Adaptive Neuro-Fuzzy Inference System," *2022 IEEE 31st International Symposium on Industrial Electronics (ISIE)*, Anchorage, AK, USA, 2022, pp. 792-798.

[17] W. Lai, H. Luo, W. Li, Y. Cao, L. Ye and Y. Wang, "Prediction of top oil temperature for oil-immersed transformer based on Kalman filter algorithm," *2017 2nd International Conference on Power and Renewable Energy (ICPRE)*, Chengdu, China, 2017, pp. 132-136.

[18] Y. Deng; J. Ruan; Y. Quan; R. Gong; D. Huang; C. Duan and Y. Xie, "A Method for Hot Spot Temperature Prediction of a 10 kV Oil-Immersed Transformer," in *IEEE Access*, vol. 7, 2019, pp. 107380-107388.

[19] J. Ruan, Y. Deng, Y. Quan and R. Gong, "Inversion Detection of Transformer Transient Hot Spot Temperature," in *IEEE Access*, vol. 9, 2021, pp. 7751-7761.

[20] R. Gong, J. Ruan, J. Chen, Y. Quan, J. Wang, and C. Duan, "Analysis and experiment of hot-spot temperature rise of 110 kV three-phase three-limb transformer," Energies, vol. 10, no. 8, pp. 1079-1091, Jul. 2017.

[21] Y. A. Çengel, Introduction to Thermodynamics and Heat Transfer, New York, NY, USA: McGraw-Hill, 2008.

[22] J. Ruan, Y. Wu, P. Li, M. Long, and Y. Gong, "Optimum methods of thermal-fuid numerical simulation for switchgear," *IEEE Access*, vol. 7, 2019, pp. 32735-32744.

[23] F. Farahmand, F. P. Dawson and J. D. Lavers, "Temperature rise and free convection heat transfer coefficient for 2-D pot-core inductors and transformers," *Fourtieth IAS Annual Meeting. Conference Record of the 2005 Industry Applications Conference, 2005.*, Hong Kong, China, 2005, pp. 2622-2629 Vol. 4.

[24] Z. Liu, R. Moorhead and J. Groner, "An Advanced Evenly-Spaced Streamline Placement Algorithm," in *IEEE Transactions on Visualization and Computer Graphics*, vol. 12, no. 5, pp. 965-972, Sept.-Oct. 2006.

[25] Dongdong Chen, "Selecting methods and its application for partners of agricultural supply chain based on Support Vector Regression," *2011 International Conference on Computer Science and Service System (CSSS)*, Nanjing, 2011, pp. 1676-1679.

[26] VAPNIK V N. *The nature of statistical learning theory*. Springer-Verlag, New York, USA ,2000.

[27] F. Xue, D. Wei, Z. Wang, T. Li, Y. Hu and H. Huang, "Grid searching method in spherical coordinate for PD location in a substation," *2018 Condition Monitoring and Diagnosis (CMD)*, Perth, WA, Australia, 2018, pp. 1-5.

[28] Qiujun Huang, Jingli Mao and Yong Liu, "An improved grid search algorithm of SVR parameters optimization," *2012 IEEE 14th International Conference on Communication Technology*, Chengdu, 2012, pp. 1022-1026.

[29] Z. Qiu *et al*., "Hybrid prediction of the power frequency breakdown voltage of short air gaps based on orthogonal design and support vector machine," in *IEEE Transactions on Dielectrics and Electrical Insulation*, vol. 23, no. 2, pp. 795-805, April 2016.

Qianyi Chen was born in Guangxi Province, China in 1991. He is currently an engineer at the Electric Power Research Institute of Guangxi Power Grid Co., Ltd. and Guangxi Power Grid Equipment Monitoring and Diagnosis Engineering Technology Research Center. His research interests include distribution automation and distribution network operation analysis.

Shaonan Chen was born in Guangxi Province, China in 1987. He is currently a senior engineer and leading technical expert at the Electric Power Research Institute of Guangxi Power Grid Co., Ltd. His research interests include intelligent patrol inspection, wireless energy transmission, big data analysis.

Weixiang Huang was born in Guangxi Province, China in 1993. He is currently an engineer at the Electric Power Research Institute of Guangxi

Power Grid Co., Ltd. and Guangxi Power Grid Equipment Monitoring and Diagnosis Engineering Technology Research Center. His research interests include lightning protection technology and operation analysis of distribution network.

Wei Zhang was born in Guangxi Province, China in 1983. He is currently a senior engineer at the Electric Power Research Institute of Guangxi Power Grid Co., Ltd. and Guangxi Power Grid Equipment Monitoring and Diagnosis Engineering Technology Research Center. His research interests include research on condition monitoring and fault diagnosis of electric power equipment, disaster prevention and mitigation of electric power system.

Kewen Li was born in Guangxi Province, China in 1979. He is currently a senior engineer at the Electric Power Research Institute of Guangxi Power Grid Co., Ltd. His research interests include distribution automation technology, power system communication technology